Reference 8

Observation of Raman emission in silicon waveguides at 1.54 μm

Ricardo Claps, Dimitri Dimitropoulos, Yan Han and Bahram Jalali

Optoelectronic Circuits and Systems Laboratory,
University of California, Los Angeles
Los Angeles, CA 90095 USA
claps@ee.ucla.edu

http://www.ee.ucla.edu/labs/ocs/

Abstract: We report the first measurements of spontaneous Raman scattering from silicon waveguides. Using a 1.43 μm pump, both forward and backward scattering were measured at 1.54 μm from Silicon-On-Insulator (SOI) waveguides. From the dependence of the Stokes power vs. pump power, we extract a value of $(4.1 \pm 2.5) \times 10^{-7}$ cm^{-1} Sr^{-1} for the Raman scattering efficiency. The results suggest that a silicon optical amplifier is within reach. The strong optical confinement in silicon waveguides is an attractive property as it lowers the pump power required for the onset of Raman scattering. The SiGe material system is also discussed.

OCIS codes: (230.7370) Waveguides; (250.3140) Integrated optoelectronic circuits; (250.4480) Optical amplifiers.

References and links

1. James B. Kuo and Shih-Chia Lin, *Low voltage SOI CMOS VLSI circuits and devices* (John Wiley and Sons, Incorporated, 2001).
2. M. Naydenkov, B. Jalali; Proceedings of the IEEE International SOI Conference, p.56, Rohnert Park, CA, October 1999.
3. S.W. Roberts, G. Pandraud, B.J. Luff, C. Bowden, P.J. Annetts, R.J. Bozeat, S. Fuller, J. Drake, M. Jackson, M. Asghari; paper 08000, NFOEC, Denver, CO, 2000.
4. M. Naydenkov, B. Jalali; Proceedings of the SPIE , Photonics West Conference, Vol. 3936, p. 33, San Jose, CA, January 2000.
5. J.M. Ralston, R.K. Chang; "Spontaneous-Raman-Scattering Efficiency and Stimulated Scattering in Silicon," Phys. Rev. B 2 1858-1862 (1970).
6. P.A. Temple, C.E. Hathaway; "Multiphonon Raman Spectrum of Silicon," Phys. Rev. B 7 3685-3697 (1973).
7. M. Cardona, "Resonance Phenomena," in *Topics in Appl. Phys. V. 50: Light Scattering in Solids II*, M. Cardona, G. Guntherodt, ed. (Springer-Verlag, Berlin, 1982).
8. T. Saito, K. Suto, J. Nishizawa, M. Kawasaki; "Spontaneous Raman scattering in [100], [110] and [11-2] directional GaP waveguides," J. Appl. Phys. **90** 1831-1835 (2001).
9. D. Dimitropoulos, R. Claps, B. Jalali; "Prospects for Raman amplification in silicon waveguides," to be presented at the Materials Research Society Fall meeting (MRS), December 6th (2002), Boston, MA. IEE Paper No.54465.
10. B. Jalali, S. Yegnanarayanan, T. Yoon, T. Yoshimoto, I. Rendina, F. Coppinger; "Advances in Silicon-on-Insulator optoelectronics," IEEE J. Sel. Top. Quantum Electron. (Special Issue on Silicon-based Optoelectronics). 4, 938-947.
11. Spectra-Physics Telecom: "Model RL5 Raman Fiber Laser Specifications."
12. R.G. Smith; "Optical Power Handling Capacity of Low Loss Optical Fibers as Determined by Stimulated Raman and Brillouin Scattering," Appl. Opt. **68** 2489-2494 (1972).
13. R.H. Stolen, E.P. Ippen; "Raman gain in glass optical waveguides," Appl. Phys. Lett. 22 276-278 (1973).
14. A.P.R. Harpin, A.G. Rickman, R.J.R. Morris, M. Asghari; US Pat. No. **6,108,478** 08/22/2000. Patent: Adiabatic Taper. Company: Bookham Technology, UK.
15. R.A. Soref; "Nonlinear refractive Index of IV-IV compound semiconductors," Appl. Opt. Vol. 31, 4627-4629 (1992).

#1680 - $15.00 US
Received September 26, 2002; Revised October 24, 2002

Report Documentation Page

Form Approved
OMB No. 0704-0188

1. REPORT DATE	2. REPORT TYPE	3. DATES COVERED
01 JUN 2005	**N/A**	**-**

4. TITLE AND SUBTITLE	5a. CONTRACT NUMBER
Observation of Raman Emission in silicon Waveguides at 1.54 UM	5b. GRANT NUMBER
	5c. PROGRAM ELEMENT NUMBER
6. AUTHOR(S)	5d. PROJECT NUMBER
	5e. TASK NUMBER
	5f. WORK UNIT NUMBER
7. PERFORMING ORGANIZATION NAME(S) AND ADDRESS(ES) **Optoelectronic Circuits and Systems Laboratory, University of California, Los Angeles, Los Angeles, California 90095-1594**	8. PERFORMING ORGANIZATION REPORT NUMBER
9. SPONSORING/MONITORING AGENCY NAME(S) AND ADDRESS(ES)	10. SPONSOR/MONITOR'S ACRONYM(S)
	11. SPONSOR/MONITOR'S REPORT NUMBER(S)

12. DISTRIBUTION/AVAILABILITY STATEMENT
Approved for public release, distribution unlimited

13. SUPPLEMENTARY NOTES
See also ADM001923.

14. ABSTRACT

15. SUBJECT TERMS

16. SECURITY CLASSIFICATION OF:			17. LIMITATION OF ABSTRACT	18. NUMBER OF PAGES	19a. NAME OF RESPONSIBLE PERSON
a. REPORT	b. ABSTRACT	c. THIS PAGE			
unclassified	**unclassified**	**unclassified**	**UU**	**9**	

16. R. Claps, D. Dimitropoulos, B. Jalali; "Stimulated Raman Scattering in Silicon Waveguides," Electronics Letters, IEE (accepted for publication, October 2002). Paper No. ELL 34761.
17. J.H. Parker, Jr., D.W. Feldman, M. Ashkin; "Raman Scattering by Silicon and Germanium," Phys. Rev. Vol. 155, 712-714 (1967).

1. Introduction

Silicon-On-Insulator (SOI) is believed to be the platform for next generation electronic Integrated Circuits (ICs) [1]. By reducing the parasitic capacitance and leakage currents, the insulating layer provided by the buried SiO_2 increases circuit speed and lowers the power consumption. At the same time, the optical waveguide properties of SOI have been recognized and exploited to the point that SOI has emerged as an attractive platform for planar lightwave circuits [2]. In this context, the availability of high quality SOI wafers and the complete compatibility with silicon Integrated Circuit (IC) technology have been prime motivations. SOI devices such as Arrayed Waveguide Gratings (AWG) and channel equalizers now compete with those realized using the silica waveguide and polymer technologies [3]. The large index mismatch between the silicon and SiO_2 allows for ultra-tight confinement of the optical field. This combined with advanced silicon patterning and etching techniques offers the possibility to realize interesting micrometer and nanometer scale photonic devices [4].

One manifestation of tight optical confinement is the enhancement of nonlinear optical effects. Because of the crystal symmetry, silicon is generally believed to be void of useable nonlinear properties. While the symmetry does prohibit 2nd order nonlinearities in bulk silicon, 3rd order phenomena do exist. Typically, 3rd order nonlinearities are too weak to be practical in integrated optical devices, because of their small sizes. One interesting exception is the Raman scattering. The Raman gain coefficient in silicon is several orders of magnitude larger than that in the amorphous glass fiber because of the single crystal structure. In addition, the tight optical confinement in an SOI waveguide will lower the threshold for Stimulated Raman Scattering (SRS). The gain bandwidth for the first-order Raman scattering is in excess of 100 GHz [5]. This makes it possible to amplify a 4 WDM channel at 25 GHz spacing. The actual bandwidth will be larger due to the convolution of the Raman gain curve with the pump linewidth.

The main feature in the spontaneous Raman spectrum of silicon corresponds to first-order Raman scattering from zone-center optical phonons [6]. It lies at 15.6 THz away from the pump and with a FWHM of 105 GHz at room temperature. The scattering efficiency in a given configuration depends on the polarization of the incident and scattered radiation with respect to the crystal orientation. Selection rules which include the wavevectors of incident and scattered radiation can then be deduced and are summarized in Table 1 [7]. Here $\hat{k}_i$ and $\hat{k}_s$ are the incident and scattered wavevectors, respectively. $\hat{e}_i$ and $\hat{e}_s$ are the corresponding polarization unit vectors, and d is the Raman tensor element [7]. The scattering efficiency is proportional to d^2. In silicon, d is the same for both LO (Longitudinal Optical) and TO (Transverse Optical) phonons, because of the degeneracy of the Γ-point LO and TO phonons. The total Raman cross section for a given geometry is then the sum of the two contributions.

#1680 - $15.00 US
Received September 26, 2002; Revised October 24, 2002

Table 1. Scattering efficiencies for different configurations in silicon. [100], [010], and [001] refer to the crystallographic directions, x, y, and z, respectively [7].

$\hat{k}_i$ & $\hat{k}_s$	$\hat{e}_i$	$\hat{e}_s$	Relative Raman efficiency
[100]	[010]	[001]	d^2
[100]	[011]	[011]	d^2
$[1\bar{1}2]$	[111]	[111]	$(4/3)d^2$
[111]	$[1\bar{1}0]$	$[1\bar{1}2]$	$(2/3)d^2$
[111]	$[1\bar{1}2]$	$[1\bar{1}2]$	d^2
$[1\bar{1}2]$	$[1\bar{1}0]$	[111]	$(1/3)d^2$

The degeneracy between the TO and LO phonons also implies a symmetry between the forward and backward scattering efficiencies in a waveguide. This is in contrast to Raman scattering in III-V compound semiconductors, where the waveguide introduces an undesired asymmetry resulting in a lower efficiency in the forward direction [8]. The symmetry between the forward and backward geometries is attractive since it allows the re-use of the pump power when it is selectively reflected back into the waveguide. This enhances the prospects for realizing an SRS based silicon amplifier or laser.

The possibility of using the Raman effect in silicon to obtain optical amplification at 1.5 μm in SOI waveguides has been proposed recently [9]. In this paper, we report the first experimental observation of Raman scattering in silicon waveguides. As a natural extension of this, we also discuss the prospects for SRS and realization of a silicon optical amplifier.

2. Experimental

The experimental setup used is shown in Fig. 1. The pump laser is a high power Cascaded-Raman-Cavity (CRC) fiber laser (Streamline-RL from Spectra-Physics). The laser delivers CW randomly-polarized light at 1427 nm, with a 2 nm linewidth. The output is collimated out of the fiber by using a lens (f = 15 mm, NA = 0.11) mounted in a precision holder with 5 degrees of freedom. In the following, this pump-launching port will be referred-to as Port 1.

#1680 - $15.00 US
Received September 26, 2002; Revised October 24, 2002

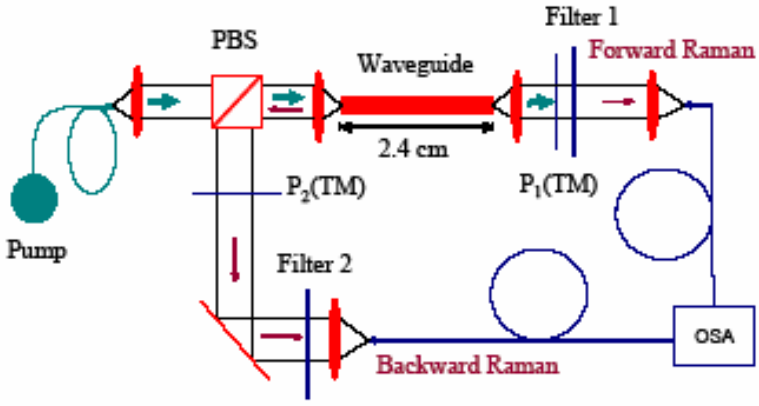

Fig. 1. Experimental setup for measurement of spontaneous Raman scattering from silicon waveguides.

A Polarization Beam Splitter (PBS) was used to split the pump beam into S and P polarized beams (Fig. 1). The P-polarized beam is sent into the waveguide and acts as the Raman pump. This polarization is preferred for the pump beam because its waveguide propagation loss is lower (by ~1 dB) than that of the TM_0-mode. The Raman signal backscattered from the waveguide is collected into Port 2 of the PBS. For further signal filtering and background rejection, a polarizer (P_2), and a 1530-1550 nm bandpass filter (Filter 2) are placed before the fiber port in Port 2. The measured value of the total back-scattering collection losses, including the PBS, the filter, the polarizer P_2 and the coupling through the fiber port into the OSA, is 15 dB.

Input and output waveguide coupling is performed by two identical, high NA microscope objective lenses (M=60X, 0.85 NA, Newport Corp.) each mounted on a stage with six-degrees-of-freedom, and with micro-positioners with <0.5 μm precision. The lens focuses the beam into a spot size of approximately 3.5 μm in diameter. The SOI waveguide chip is mounted on a vacuum chuck and its position is adjusted using an XY stage. A polarizer (P_1) and a bandpass filter (Filter 1) remove the pump signal and pass the forward scattered radiation.

The SOI rib waveguide used is shown in Fig. 2. It was fabricated on a [100] SOI substrate with the waveguide oriented along one of the in-plane crystallographic axis [100]. The waveguide has a 5μm width, and 2.5μm rib height, with a 5μm total thickness [10]. Beam Propagation Method (BPM) simulations show that the overlap between the TE_0 (pump) and TM_0 (signal) modes in the waveguide is better than 95%. The simulations were carried out using a commercially available software (BeamProp, RSoft Corporation). The polarization mode crosstalk (TE to TM conversion) for this waveguide is measured to be -18 dB. This is a negligible quantity in terms of loss of pump power for Raman scattering compared to waveguide coupling losses. Still, it introduces a background signal that may become important and needs to be taken into account in the spectral analysis, especially when the laser is operating at maximum power. The reason for this polarization mode conversion is due to imperfections in waveguide fabrication, since BPM simulations on the waveguide design show a much smaller value. The measured total losses for this waveguide are 11.5 dB for the TE_0-mode and 12.3 dB for the TM_0-mode. These include the coupling losses (input plus output) Fresnel reflections, and the propagation loss. The input waveguide facet was not Anti Reflection (AR) coated. Doing so will reduce the pump losses by approximately 1.5 dB.

#1680 - $15.00 US
Received September 26, 2002; Revised October 24, 2002

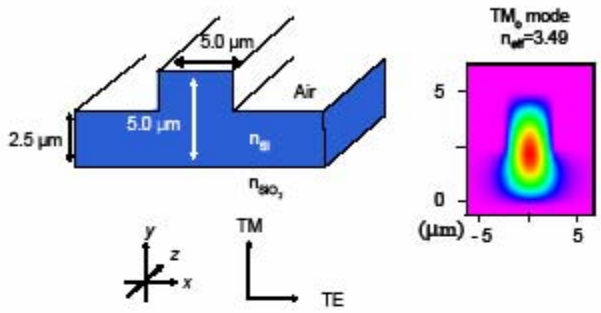

Fig. 2. SOI Waveguide used. The (x, y, z) coordinates are oriented along the crystallographic axes. The resulting TM_0 mode (λ=1.54 μm) from a BPM calculation is depicted to the right. The effective index of refraction is calculated assuming n=3.5 for bulk silicon.

By measuring the FWHM of the power coupled out of the waveguide as a function of z (the distance from the output facet along the optical axis) the angular dispersion is found to be $\theta_V = 22^o$, in the vertical direction, and $\theta_H = 8^o$ in the horizontal direction. Using these values and Snell's law for silicon/air interface, the solid angle of collection within the waveguide can be calculated to be 0.013 Sr.

3. Results

The Raman spectra were measured for both forward and reverse scattering geometries. The pump polarization was oriented parallel to the polarization of the TE_0 waveguide mode. All measurements were performed at room temperature. In order to establish the fact that the observed emission is from the waveguide and not from bulk silicon, measurements were repeated for different offsets of the waveguide relative to the optical axis. The measured spectra are shown in Fig. 3. The spectra, measured along the polarization of the TM_0 waveguide mode, show a peak at 1542 nm, corresponding to a 15.7 THz red-shifted from the pump wavelength. These observations are in excellent agreement with the value of the optical phonon frequency in silicon.

#1680 - $15.00 US

Received September 26, 2002; Revised October 24, 2002

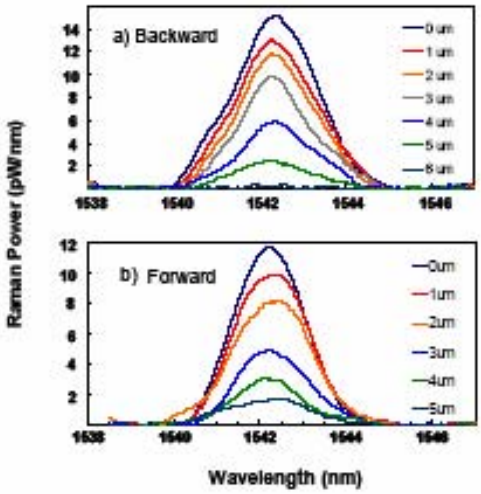

Fig. 3. Raman spectra from silicon obtained for different horizontal offsets of the waveguide relative to the optical axis. Fig. 3a shows the back-scattered spectra, and Fig. 3b shows the forward-scattered spectra.

The spectral width of 350 GHz is the convolution of the silicon Raman linewidth, 105 GHz, and the 250 GHz (non-Gaussian) linewidth of the pump laser. Figure 4 shows the measured spatial profile for the Raman emission, along with BPM simulated mode profiles for the TM_0 mode of the waveguide. Assuming Gaussian spatial profiles, values of 3.8 ± 0.5 μm for the horizontal distribution and 2.3 ± 0.5 μm for the vertical distribution are obtained. The vertical measured profile is in excellent agreement with the BPM simulation, although the horizontal profile deviates by approximately 25%. This can be attributed to the uncertainty in the width of the rib section caused by undercutting during the etching process.

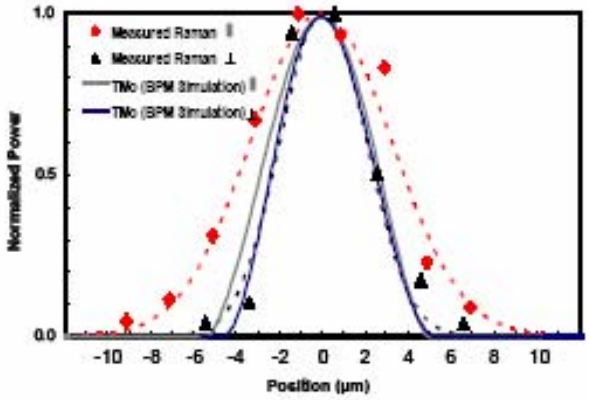

Fig. 4. Measured profiles of the Raman emission from the SOI waveguide in horizontal (∥ or x in Fig. 2), and vertical (⊥ or y in Fig. 2) directions. The corresponding TM_0 mode profiles, calculated using BPM simulations, are super-imposed for comparison. Dashed lines are Gaussian fits to the data.

#1680 - $15.00 US
Received September 26, 2002; Revised October 24, 2002

Figure 5 shows the Raman spectra, measured in the forward scattering geometry at the output end of the waveguide, as a function of pump laser power. The pump laser power was measured after the PBS (Fig. 1) and before the waveguide coupling optics. The observed broadening of the linewidth at higher pump powers is due to the broadening of the pump laser linewidth. This is a well documented effect for the pump laser used [11].

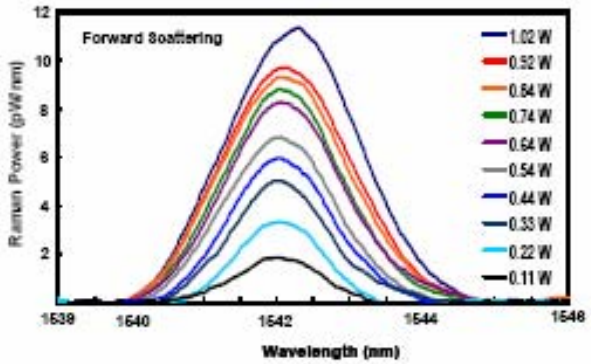

Fig. 5. Raman spectra measured for different values of pump power.

Figure 6 shows the integrated Raman power versus pump power for both the forward and the backward scattering geometries. As expected, the spontaneous emission power has a linear dependence on the pump power. There is a slight difference in slopes which can be accounted for by the waveguide propagation loss, as shown below. By comparing the Raman power in the forward and backward directions, both the spontaneous scattering efficiency and the waveguide propagation loss can be extracted. This procedure is outlined below.

In the case of spontaneous Raman scattering, the equations that govern the propagation of pump ($P_P(z)$) and signal ($P_R(z)$) field power along the waveguide are obtained in a manner similar to [12] but with the effect of the stimulated emission term omitted. Therefore,

$$P_p(z) = P_p(0)\, e^{-\gamma z}. \tag{1}$$

$$\frac{dP_R(z)}{dz} = \mp \gamma P_R(z) \pm \alpha\, P_p(z). \tag{2}$$

Where the upper (lower) sign in Equation 2 applies in forward (backward) scattering. Here, γ is the propagation loss of the waveguide in units of cm^{-1}, and α is the spontaneous Raman coefficient for the silicon waveguide, defined as:

$$\alpha = S\,\Delta\Omega. \tag{3}$$

With S the Raman scattering efficiency ($cm^{-1}Sr^{-1}$) in silicon at 1542 nm, and $\Delta\Omega$ is the effective solid angle of collection for the TM_0 waveguide mode and is $\Delta\Omega = 0.013$ Sr. The

#1680 - $15.00 US

Received September 26, 2002; Revised October 24, 2002

total Raman signal power, P_R, measured either in forward configuration (at the output end of the waveguide) or in backward configuration (from Port 2 in the PBS) is related to the pump power at the input facet of the waveguide (P_P) as:

Backward:
$$P_R = \alpha \left\{ \frac{1 - e^{-2\gamma L}}{2\gamma} \right\} P_P . \tag{4}$$

Forward:
$$P_R = \alpha L e^{-\gamma L} P_P . \tag{5}$$

Where L is the length of the waveguide. From (4) and (5), it is seen that the ratio between the slopes of the lines in Fig. 7, m, can be related to γ (in the low propagation loss limit) by

$$m = \frac{\sinh(\gamma L)}{\gamma L} \tag{6}$$

With the value of m obtained from Fig. 6 and using Equation (6), we get an estimate for the propagation loss, $\gamma = 0.64$ cm^{-1} = 2.8 dB/cm. Note that the value thus obtained is independent of the Raman scattering coefficient and the optical coupling efficiency. Including this value of γ into Equation (4) and using the measured slope in Fig. 6, with further correction for the back-scatter collection losses (15 dB) and waveguide coupling losses (4 ± 2 dB), we obtain $\alpha = (5.3 \pm 3.2) \times 10^{-9}$ cm^{-1}. With the above value for $\Delta\Omega$ (0.013 Sr), the scattering efficiency in silicon is obtained to be $S = (4.1 \pm 2.5) \times 10^{-7}$ cm^{-1} Sr^{-1}. Ralston and Chang [5] have obtained a value for S from backscattering measurements on bulk silicon and at a pump wavelength of 1.06 μm. Since the 1 to 1.5 μm region is far from any resonances, there will only be a λ^{-4} dependence of S on wavelength. This results in a value $S = 8.4 \times 10^{-7}$ cm^{-1} Sr^{-1} at 1.54 μm from reference [5] in good agreement with the results reported here.

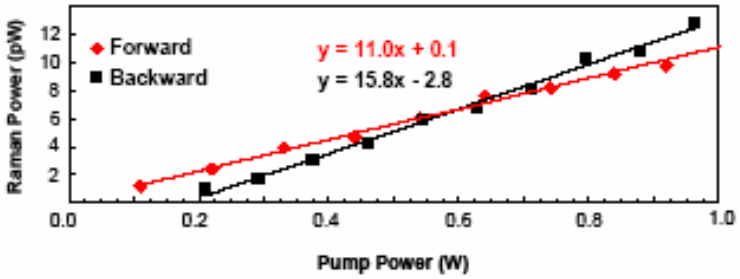

Fig. 6. Spontaneous Raman intensity as a function of pump power. Forward and backward scattering cases are shown. The pump power was measured between the PBS and the input coupling lens.

4. Prospects for Stimulated Raman Scattering (SRS) in Silicon

A key issue in obtaining SRS will be the required pump power. To obtain a first-order estimate for the pump power needed to observe signal amplification, we consider an SOI

#1680 - $15.00 US
Received September 26, 2002; Revised October 24, 2002

waveguide with cross sectional area of 1μm x 1μm and a length of 2cm. The role of the waveguide in confining the pump intensity and propagating it through the material with a low loss is crucial to enhance the Raman scattered signal. The analysis for SRS in the silicon waveguide is analogous to that for fiber Raman amplification. The amplified Raman power, $P_R(L)$ after a length L, is given as [13]

$$P_R(L) = P_R(0)\exp(-\gamma L + \frac{g_s S_P(0)}{\gamma}(1-\exp(-\gamma L))). \qquad (7)$$

Where γ is the measured propagation loss (2.8 dB/cm), and $S_P(0) = P_P(0)/A$, where $P_P(0)$ is the input pump power, and A is the modal overlap between the propagating TE_0 and TM_0 waveguide modes. The stimulated Raman gain coefficient, g_s, in units of m/W is [5]

$$g_s = \frac{8\pi c^2 \omega_p}{\hbar \omega_s^4 n^2(\omega_s)(N+1)\Delta\omega} S. \qquad (8)$$

Where N is the Bose occupation factor (0.1 at room temperature), n is the refractive index, ω_p and ω_s are the pump and Stokes frequencies, respectively, and $\Delta\omega$ is the FWHM of the spontaneous lineshape. Substituting the appropriate values, we obtain $g_s = 0.076$ cm/MW.

The result of Equation (7) suggests that a CW pump power of 180 mW at the front facet of an AR-coated waveguide would be the threshold for stimulated amplification. Threshold is defined as the pump power required to achieve optical transparency at the signal wavelength. Since the threshold pump power depends on the waveguide loss, one challenge in practical realization of a silicon Raman amplifier will be fabrication of low loss waveguides with small cross sectional dimensions. The other challenge will be efficient coupling of pump power into such waveguides. To this end, a recent demonstration of SOI waveguides with tapered couplers is an attractive development [14].

An alternative silicon-based waveguide is the $Si/Si_xGe_{1-x}/Si$ system. It has been suggested by Soref [15] that Two Photon Absorption (TPA) could be twenty-times larger in Ge than in silicon. In the context of Raman amplification, this is highly undesirable since TPA causes pump depletion [16]. Furthermore, the measured Raman efficiencies for Si are a factor of 10 times larger than that of Ge at 488 nm [17], but no experimental data exists for the Raman susceptibility at the low frequency limit for Ge and so accurate comparison cannot be made without further investigation.

5. Summary

In summary, we have reported the first measurements of Raman emission from silicon waveguides. Both forward and backward scattering were measured at 1.54 μm. From the dependence of the Stokes power vs. pump power, we extract a value of $(4.1 \pm 2.5) \times 10^{-7}$ cm^{-1} Sr^{-1} for the Raman scattering efficiency. Based on this value, prospects for stimulated Raman scattering were analyzed. The results suggest that a silicon Raman amplifier is possible. The main challenges for realization of a practical device will be to attain a low waveguide propagation loss and a high pump coupling efficiency.

Acknowledgments

The authors would like to acknowledge Prof. Jia-Ming Liu of UCLA for helpful discussions, and Dr. Jag Shah of DARPA for his support.

#1680 - $15.00 US Received September 26, 2002; Revised October 24, 2002